Nonimmobilized Enzyme Kinetics That Rely on Laminar Flow

Kenichi Yamashita,[†] Masaya Miyazaki,[‡] Hiroyuki Nakamura,[†] and Hideaki Maeda*[,†,‡,§]

Micro- & Nano-space Chemistry Group, Nanotechnology Research Institute, National Institute of Advanced Industrial Science and Technology (AIST), 807-1, Shuku-machi, Tosu, Saga 841-0052, Japan, Graduate School of Engineering Sciences, Kyushu University, 6-1, Kasuga-Kouen, Kasuga, Fukuoka 816-8580, Japan, and JST, CREST, 807-1, Shuku-machi, Tosu, Saga 841-0052, Japan

Received: September 27, 2008; Revised Manuscript Received: November 17, 2008

This paper describes kinetic parameters of an enzymatic reaction obtained by measuring the reaction rates of hydrolysis by trypsin at various flow rates and temperatures. Using these parameters, the mechanisms of an efficient reaction of nonimmobilized, i.e., "free state" enzyme in microchannel laminar flow can be examined from a kinetic perspective. Efficient complex formation between the enzyme and substrate was confirmed through Michaelis−Menten analysis. Results show that the enhancing effect of microfluidics in complex formation accelerated the enzymatic reaction. Results of activation energy analysis confirmed that a decrease in the apparent activation energy occurred as the flow rate increased. Taken together, these results suggest that a microfluidic system is useful for performing rapid reactions by influencing the complex formation and activation energy.

Introduction

The microchannel environment, as defined by the laminar nature of fluid flow, differs greatly from that of a batchwise system. In the latter, solvent molecules interact with solutes isotropically. In contrast, interaction of solutes with solvents in a microchannel laminar flow is nonisotropic, suggesting that such behavior is a characteristic of solutes under laminar conditions. Consequently, chemical reactivity in microchannel laminar flow often differs from that of a batch system. Macromolecule dynamics of different materials in fluid flow have been well studied. In particular, conformations of polymer molecules such as DNA strands under flows of various kinds are studied.[1−9] Such an approach enables easy observation and supports theoretical discussion. Theoretically and experimentally, it has been confirmed that DNA strands, which form a coiled state in a bulk solution, stretch or form various shapes in shear[1,2] and elongational[2,3] flow. We have reported stretching and orientation of DNA strands in a microchannel laminar flow through direct observation[4] and linear dichroism (LD) spectra measurements.[5] Our results conform to those obtained from theoretical studies of coil-stretch transition[6] and relaxation time[7] of polymer molecules. According to these theoretical studies,[6,7] possibilities of conformational changes of solute molecules in a fluid are not dependent on solute molecular species, but rather on the molecular size of the solutes and fluid conditions. Therefore, aside from DNA strands, results of these theoretical studies are readily applicable to macromolecules such as enzymes or proteins under comparatively slow flow rates.

To explore details of the changes in chemical reactivity in microfluidic reactor, we examined the influence of microchannel laminar flow on chemical reactivity from a physicochemical perspective.[5,8] We have reported the shift in thermal stability of DNA duplex in a microchannel laminar flow, along with its dependence on flow rate.[5,8] Moreover, based on thermodynamic analysis, the change in conformational entropy caused by microfluidic stretching and orientation of DNA strands is an important factor in microfluidic thermal stability shift.[5,8] Using kinetic analysis, we have also confirmed the change of activation energy of DNA duplex-coil equilibrium in microchannel laminar flow and its dependence on the flow rate.[9] These results suggest the potential application of microreactors as a chemical-reactivity-regulating device. The enhancing effect of the microreactor is simply regulated by the flow rate. Moreover, the microreactor is a useful platform for enzymatic reactions.[10] Enzymatic reactions using microreactors provide many advantages such as low reagent consumption and efficient reactions through a high surface-to-volume ratio and accurate temperature controllability.[10−12] Microreactors using enzymatic reactions are classified into two types: enzyme-immobilization-based microreactors and nonimmobilization-based microreactors. Many reports of microreactors using enzymatic reactions exist; most such microreactors use enzyme immobilization on a microchannel wall or beads. This enzyme immobilization method presents advantages that include the efficient use of enzymes, in addition to several disadvantages such as the difficulty of inactivated enzyme replacement and reduced enzymatic activity because of an altered enzyme conformation and steric hindrance of the catalytic site.[10,11]

For enzymes of various kinds, the kinetic parameters in immobilized enzymatic reactions using microreactors have been reported.[11,12] According to these reported results, differences in both Michaelis constants, K_m and the turnover rate, k_{cat} exist between the microfluidic system and batchwise system. These K_m values of microfluidic reactions of immobilized enzymes were both higher and smaller than those of the batch system. In contrast to K_m values, all k_{cat} values of microfluidic reactions of immobilized enzymes were smaller than those of the batchwise system. The reduced k_{cat} values in immobilized enzymatic reactions using a microreactor are caused by an

* Corresponding author. Telephone: +81-942-81-3676. Fax: +81-942-81-3657. E-mail: maeda-h@aist.go.jp.
† Micro- & Nano-space Chemistry Group, Nanotechnology Research Institute, National Institute of Advanced Industrial Science and Technology (AIST).
‡ Graduate School of Engineering Sciences, Kyushu University.
§ JST, CREST.

10.1021/jp808572a CCC: $40.75
Published on Web 12/10/2008

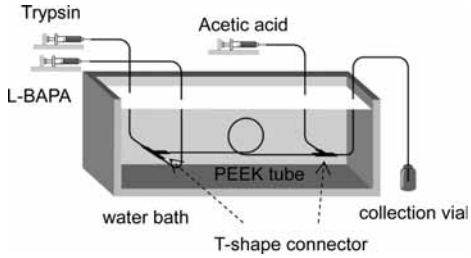

Figure 1. Schematic showing the experimental setup used for reaction rate measurements of L-BAPA hydrolysis by trypsin.

altered enzyme conformation and steric hindrance of the catalytic site.[11]

Our study specifically addressed the fundamental behavior of the nonimmobilized enzyme reactor, i.e., enzymes in a "free state", and change in chemical reactivity under microchannel laminar flow. Furthermore, the reaction rates of some "free state" enzymes are higher using the microreactors than the batchwise enzymatic reactions.[13,14] On the other hand, kinetic analysis has often been used to elucidate chemical reaction mechanisms and has elicited valuable knowledge related to the control of chemical reactions. Therefore, in this study, we examine the influence of microchannel laminar flow on the chemical reactivity of "free state" enzymes from a kinetic perspective.

Experimental Methods

Chemicals. Trypsin (from bovine pancreas; EC 3.4.21.4) and acetic acid were used (Wako Pure Chemical Industries Ltd., Japan), in addition to benzoyl-L-arginine-*p*-nitroanilide (L-BAPA; Peptide Institute Inc., Japan). These reagents were dissolved separately in aqueous solutions of phosphate buffered saline (pH 7.4). In all experiments, the concentrations of trypsin and acetic acid were constant: 0.5 μM trypsin and 30% (v/v) acetic acid. The L-BAPA concentrations were different for each experiment.

Apparatus. Figure 1 depicts a schematic representation of the experimental setup for the measurement of the reaction rate of L-BAPA hydrolysis by trypsin. In all experiments, three aqueous solutions of trypsin, L-BAPA, and acetic acid were injected using a multisyringe pump (PHD2000; Harvard Apparatus, Holliston, MA) at the same flow rate. The trypsin solution and L-BAPA solution were injected separately into a polyether ether ketone (PEEK) tube (250 μm internal diameter). Hydrolysis of L-BAPA was started by mixing in a T-shaped connector. This hydrolysis reaction was terminated by the addition of acetic acid solution. The reaction temperature was controlled by soaking the PEEK tube in a water bath (F25; Julabo Labortechnik GmbH, Germany). The reaction was evaluated as the amount of released *p*-nitroaniline calculated from the absorbance at 405 nm using a spectrophotometer (U-560; Jasco Inc. Japan). The extinction coefficient of *p*-nitroaniline at 405 nm is 9,920 cm^{-1} M^{-1}.[15] In kinetic analysis, the concentration parameters of trypsin and L-BAPA after mixing of these solutions, and *p*-nitroaniline before addition of acetic acid were used.

Michaelis−Menten Analysis. Under the condition of constant temperature at 30 °C, the experiments were carried out at 2.0−34 mm s^{-1} with L-BAPA concentrations at 10−0.05 mM using various PEEK tube lengths of 0.25−8 m between two T-shaped connectors. The residence times were defined as the reaction times calculated from the flow rates and PEEK tube lengths. In addition, batchwise reaction was also measured; those measurements were used as control data. The reaction rate was obtained from the slope of the plots of reaction time against the released *p*-nitroaniline concentration at each flow rate and L-BAPA concentration.

The Michaelis−Menten equation was used to evaluate the kinetics of this enzymatic reaction as described below.[16]

On the basis of our experiments using sufficiently high substrate concentration in comparison to enzyme concentration, the Michaelis−Menten equation yields the following.

$$V = \frac{V_{max}[S]_0}{K_m + [S]_0} \quad (1)$$

In this equation, V represents the rate of enzymatic reaction, V_{max} represents the maximum rate, i.e., the rate of reaction at which the active sites of enzyme are saturated with the substrate; $[S]_0$ represents the initial concentration of the substrate, and K_m represents the Michaelis−Menten constant. The Hanes−Woolf equation (eq 2) yields V_{max} and K_m.

$$\frac{[S]_0}{V} = \frac{1}{V_{max}}[S]_0 + \frac{K_m}{V_{max}} \quad (2)$$

Therefore, V_{max} and K_m are obtainable from plots of $[S]_0/V$ against $[S]_0$ representing V_{max} = 1/(slope) and $K_m = V_{max} \times$ (y-intercept).

The turnover rate, k_{cat}, is obtainable from eq 3.

$$V_{max} = k_{cat}[E]_0 \quad (3)$$

In this equation, $[E]_0$ represents the initial enzyme concentration.

Determination of Activation Energies. Under the condition of constant substrate concentration at 10 mM and PEEK tube length of 2 m between two T-shape connectors, the experiments were conducted at flow rates of 2.0−34 mm s^{-1} and reaction temperatures of 8−35 °C. In addition, batchwise reaction data were used as control data. The reaction rates were obtained from these experiments under their respective flow rates and reaction temperatures. The activation energies of this enzymatic reaction were evaluated using the Arrhenius equation portrayed below.

An enzymatic reaction might be represented as shown below:

$$E + S \underset{}{\overset{}{\rightleftharpoons}} ES \xrightarrow{k_{app}} E + P \quad (4)$$

In that expression, P represents the product of this reaction and k_{app} represents the apparent rate constant. In this study involving the use of flow-type reactor and short reaction time, the enzyme concentration can be considered constant, which is actually equal to the initial concentration. Therefore, the rate equation yields the following equation.

$$\frac{d[P]}{dt} = k_{app}[E]_0[S]_0 \quad (5)$$

The apparent activation energy E_a can be determined using the Arrhenius equations.[17]

$$\ln(k_{app}) = -\frac{E_a}{RT} \quad (6)$$

That equation is expressed by the slope of the plot of $\ln(k_{app})$ as a function of $1/T$, where R is the gas constant.

Results and Discussion

The fluid flow in a PEEK tube is characterized as laminar. Its velocity distribution is parabolic, as defined using the

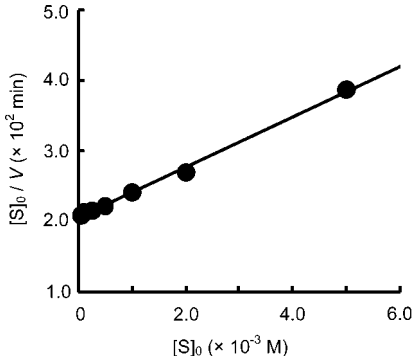

Figure 2. A Hanes−Woolf plot showing a 10 mm s^{-1} flow rate. The line shows least-squares fitting of the data. Hanes−Woolf plots of all flow rate conditions are shown in the Supporting Information.

Hagen−Poiseuille equation.[18] At a 34 mm s^{-1} flow rate and 35 °C temperature, the corresponding Reynolds number is about 12. Therefore, the flow is classified as laminar. Other experimental conditions used in this study show characteristics of a laminar flow, with a Reynolds number lower than 12.

To examine the influence of microchannel laminar flow on chemical reactivity of "free state" enzymes, we selected trypsin as the target enzyme. Trypsin is a well-reported enzyme used as a model for enzymatic reactions in a microreactor based on both immobilized and nonimmobilized methods; its kinetic parameters, including the Michaelis−Menten method and the Arrhenius plot, have been reported.[19,20] Additionally, it has been reported that the reaction rate of trypsin using the microreactor was higher than for bulk scale enzymatic reactions.[13] On the other hand, the use of L-BAPA enables simple quantitative determination using the previously reported method.[15]

Michaelis−Menten analysis is a well-known kinetics analysis for the study of enzymes. It has often been used for elucidation of mechanisms in enzymatic reactions. For that reason, we specifically examined the Michaelis−Menten analysis of L-BAPA hydrolysis by trypsin. Herein, under constant temperature at 30 °C, the experiments were carried out at various flow rates and different substrate concentrations using various PEEK tube lengths. The reaction rate was obtained from the slope of the plots of the released *p*-nitroaniline concentration against reaction time at each flow rate and L-BAPA concentration (The plots of the released *p*-nitroaniline concentration against reaction time at 1 mM L-BAPA are shown in the Supporting Information). These plots portrayed good linearity for all plots: $R^2 > 0.97$.

In this study, the Michaelis−Menten constant, K_m and maximum rate, V_{max} were determined using the Hanes−Woolf equation. In order to avoid the errors in low $[S]_0$ range, we chose the Hanes−Woolf equation. Figure 2 shows the Hanes−Woolf plot at the flow rate of 10 mm s^{-1} as an example. The Hanes-Woolf plots of all flow rate conditions are shown in the Supporting Information. In all flow rate conditions, Hanes-Woolf plots showed good linearity for all plots: $R^2 > 0.98$. This high linearity verifies that the Michaelis−Menten model is applicable to the enzymatic reaction used in this study.[16] The turnover rate, i.e. catalytic activity, k_{cat} is obtained from eq 3; the catalytic efficiency k_{cat}/K_m is calculated. The obtained values for the kinetic parameters are presented in Table 1. These values are in agreement with the previously reported kinetic parameters of trypsin-catalyzed hydrolysis.[19,20] Figure 3 shows plots of these kinetic parameters against the flow rate. Both V_{max} and k_{cat} were almost constant for all flow rates. In contrast, K_m showed a decreasing trend as the flow rate increased; an increasing trend was apparent in k_{cat}/K_m as the flow rate increased. A decrease in K_m indicates more efficient complex formation between enzyme and substrate. These flow-rate-dependent changes indicate that such changes are induced by microchannel laminar flow. Similar with DNA duplex behavior in microchannel

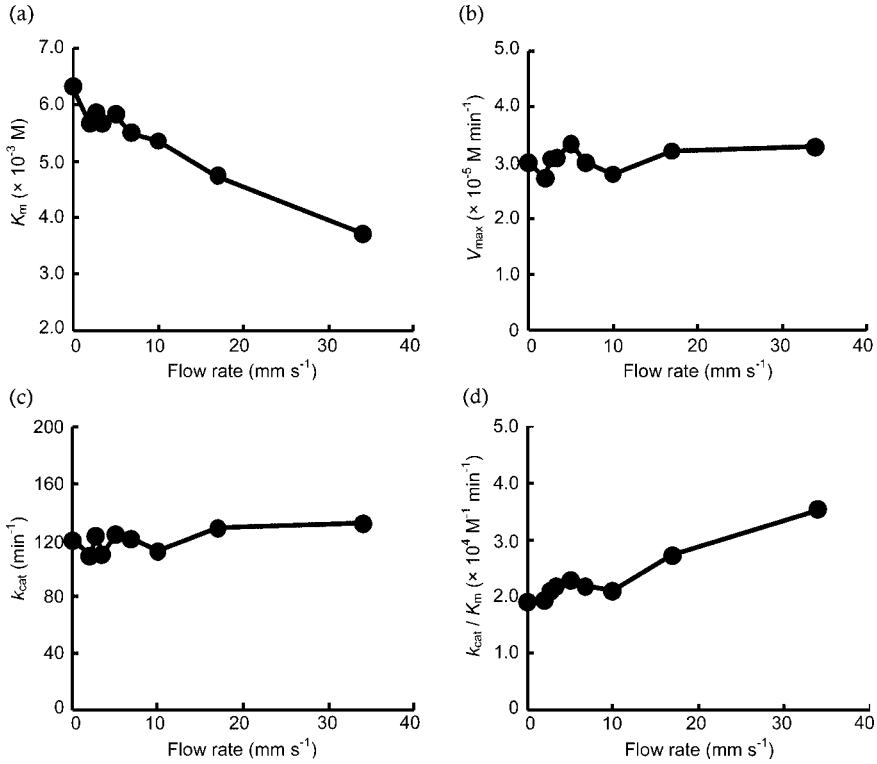

Figure 3. Plots of the kinetic parameters against the flow rate: (a) K_m, (b) V_{max}, (c) k_{cat}, and (d) k_{cat}/K_m vs the flow rate. The point of batchwise reaction is plotted at 0 mm s^{-1}.

TABLE 1: Kinetic Parameters for the Trypsin-Catalyzed Hydrolysis of BAPA[a]

flow rate, mm s^{-1}	$K_m \times 10^{-3}$ M	$V_{max} \times 10^{-5}$ M min^{-1}	k_{cat}, min^{-1}	$k_{cat}/K_m \times 10^4$ $M^{-1}s^{-1}$	E_a, kcal mol^{-1}
batchwise	6.31	3.01	120	1.91	9.41
2.0	5.67	2.73	109	1.93	9.47
2.7	5.84	3.08	123	2.11	
3.4	5.67	3.09	110	2.18	9.32
5.1	5.83	3.35	124	2.30	9.33
6.8	5.50	3.01	121	2.19	9.16
8.5					8.76
10	5.35	2.80	112	2.10	
12					7.64
17	4.74	3.22	129	2.72	6.70
24					5.85
34	3.72	3.29	132	3.53	4.40

[a] Estimation of errors: These values were determined from observed reaction rates. Errors for the reaction rates were 8% for batchwise and 11% for flow state reactions.

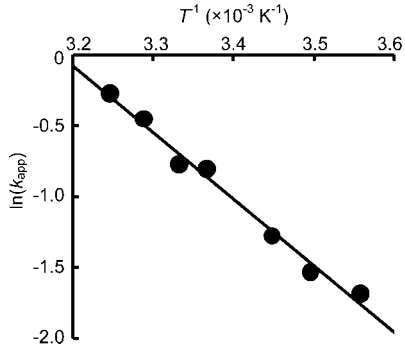

Figure 4. Arrhenius plot of a 3.4 mm s^{-1} flow rate. The line shows least-squares fitting of the data. Arrhenius plots of all flow rate conditions are shown in the Supporting Information.

laminar flow,[4,5,8] we consider the change of orientation of trypsin molecule as a key factor in the change of K_m. According to the previous reports,[6,8] the trypsin molecule has sufficient size that supports the necessary orientation for reaction to occur in microchannel laminar flow. In addition to the effect of efficient complex formation, in contrast to the enzyme-immobilization method, it is considered important that the catalytic activity of "free state" enzyme is not decreased by an altered enzyme conformation and steric hindrance of the catalytic site.

On the other hand, we examined the activation energy of enzymatic reaction in microchannel laminar flow and viewed from another kinetic perspective. Herein, under constant substrate concentration at 10 mM and PEEK tube length of 2 m, the experiments were carried out at various flow rates and various temperatures. The reaction temperature range of 8−35 °C is lower than the optimum temperature of trypsin. Therefore, the influence of inactivation is excluded.[20] The apparent rate constants k_{app}s were obtained from the reaction rates at each reaction temperature and flow rate. The apparent activation energies E_as were obtained from the Arrhenius plot at each reaction temperature. Figure 4 shows the Arrhenius plot at the flow rate of 3.4 mm s^{-1} as an example. The Arrhenius plots of all flow rate conditions are shown in the Supporting Information. For all flow rate conditions, Arrhenius plots indicated good linearity for all plots: $R^2 > 0.98$. The obtained E_a values are also presented in Table 1. Figure 5 shows the plot of E_a values against the flow rate. In contrast to the almost constant E_a values at the slower flow rate, a decrease in E_a was observed at faster flow rates. The flow-rate-dependent changes in E_a indicate that acceleration of enzymatic reaction results from microchannel laminar flow.

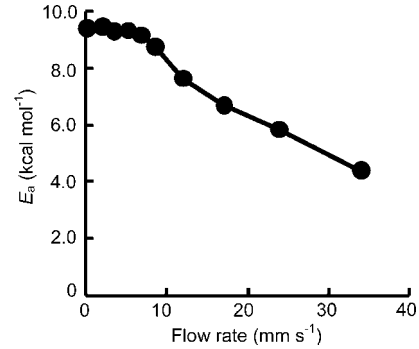

Figure 5. Plot of E_a values against the flow rate. The point of batchwise reaction is plotted at 0 mm s^{-1}.

Conclusion

In conclusion, we described the kinetic parameters of the enzymatic reaction by measuring the reaction rates of hydrolysis by trypsin at various flow rates and temperatures to examine the mechanism of efficient reaction of "free state" enzyme in microchannel laminar flow from a kinetic perspective. The efficient complex formation between enzyme and substrate was confirmed using Michaelis−Menten analysis. Results of the analysis showed the enhancing effect of microfluidics in a complex formation, which provided an acceleration of the enzymatic reaction. Furthermore, in contrast to the enzyme-immobilization method, it is an important factor that the catalytic activity of "free state" enzyme is not decreased by altered enzyme conformation and steric hindrance of the catalytic site. On the other hand, the activation energy analysis results confirmed that a decrease in apparent activation energy was observed as the flow rate increased. The enhancing effect of microfluidics in such reactions is regulated simply by the flow rate. Therefore, these results suggest that a microfluidic system is useful for performing rapid reactions by influencing the complex formation and activation energy. We earlier reported the possibility of controlling chemical reactivity using microfluidics in our study of the fundamental behavior of DNA strands and measurements of their physicochemical properties.[5,8,9] In addition to earlier theoretical studies using DNA strands, this study, which demonstrates the capability of controlling an enzymatic reaction by microfluidics, provides proof of chemical reactivity control by microfluidics. We consider the results of this study not only as a contribution to the improvement of microreactors but also as a valuable contribution to information related to the function and design of chemical reactors in general.

Acknowledgment. This work was funded by a Grant-in-Aid for Young Scientists (A) (No. 20686054) from the Ministry of Education, Culture, Sports, Science and Technology. We thank Dr. Yoshiko Yamaguchi of AIST for helpful discussion.

Supporting Information Available: Figures showing plots of the released *p*-nitroaniline concentration against reaction time at 1 mM L-BAPA, the Hanes−Woolf plots of batchwise and all flow rate conditions, and Arrhenius plots for batchwise and all flow rate conditions. This material is available free of charge via the Internet at http://pubs.acs.org.

References and Notes

(1) (a) LeDuc, P.; Haber, C.; Bao, G.; Wirtz, D. *Nature* **1999**, *399*, 564–566. (b) Hur, J. S.; Shaqfeh, E. S. G. *J. Rheol.* **2000**, *44*, 713–742.

(2) (a) Larson, R. G. *J. Non-Newtonian Fluid Mech.* **2000**, *94*, 37–45. (b) Wong, P. K.; Lee, Y.; Ho, C. *J. Fluid. Mech.* **2003**, *497*, 55–65.

(3) (a) Keller, A.; Odell, J. A. *Colloid Polym. Sci.* **1985**, *263*, 181–201. (b) Reese, H. R.; Zimm, B. H. *J. Chem. Phys.* **1990**, *92*, 2650–2662. (c) Sasaki, N.; Hayakawa, I.; Hikichi, K.; Atkins, E. D. T. *J. Appl. Polym. Sci.* **1996**, *59*, 1389–1394. (d) Smith, D. E.; Chu, S. *Science* **1998**, *281*, 1335–1340. (e) Larson, R. G.; Hu, H. *J. Rheol.* **1999**, *43*, 267–304. (f) Duggal, R.; Pasquali, M. *J. Rheol.* **2004**, *48*, 745–764. (g) Larson, J. W.; Yantz, G. R.; Zhong, Q.; Charnas, R.; Antoni, C. M. D.; Gallo, M. V.; Gillis, K. A.; Neely, L. A.; Phillips, K. M.; Wong, G. G.; Gullans, S. R.; Gilmanshin, R. *Lab Chip* **2006**, *6*, 1187–1199.

(4) (a) Yamashita, K.; Yamaguchi, Y.; Miyazaki, M.; Nakamura, H.; Shimizu, H.; Maeda, H. *Chem. Lett.* **2004**, *33*, 628–629. (b) Yamashita, K.; Yamaguchi, Y.; Miyazaki, M.; Nakamura, H.; Shimizu, H.; Maeda, H. *Anal. Biochem.* **2004**, *332*, 274–279.

(5) Yamashita, K.; Miyazaki, M.; Yamaguchi, Y.; Nakamura, H.; Maeda, H. *ChemPhysChem.* **2007**, *8*, 1307–1310.

(6) DeGennes, P. G. *J. Chem. Phys.* **1974**, *60*, 5030–5042.

(7) Zimm, B. H. *J. Chem. Phys.* **1956**, *24*, 269–278.

(8) Yamashita, K.; Miyazaki, M.; Yamaguchi, Y.; Nakamura, H.; Maeda, H. *J. Phys. Chem. B* **2007**, *111*, 6127–6133.

(9) Yamashita, K.; Miyazaki, M.; Yamaguchi, Y.; Nakamura, H.; Maeda, H. *Lab Chip* **2008**, *8*, 1171–1177.

(10) Miyazaki, M.; Maeda, H. *Trends Biotechnol.* **2006**, *24*, 463–470.

(11) Kerby, M. B.; Legge, R. S.; Tripathi, A. *Anal. Chem.* **2006**, *78*, 8273–8280.

(12) (a) Lilly, M. D.; Hornby, W. E.; Crook, E. M. *Biochem. J.* **1966**, *100*, 718–723. (b) Mao, H.; Yang, T.; Cremer, P. S. *Anal. Chem.* **2002**, *74*, 379–385. (c) Seong, G. H.; Heo, J.; Crooks, R. M. *Anal. Chem.* **2003**, *75*, 3161–3167. (d) Gleason, N. J.; Carbeck, J. D. *Langmuir* **2004**, *20*, 6374–6381. (e) Koh, W. G.; Pishko, M. *Sens. Actuators B* **2005**, *106*, 335–342. (f) DeLouise, L. A.; Miller, B. L. *Anal. Chem.* **2005**, *77*, 1950–1956. (g) Liu, A.-L.; Zhou, T.; He, F.-Y.; Xu, J.-J.; Lu, Y.; Chen, H.-Y.; Xia, X.-H. *Lab Chip* **2006**, *6*, 811–818.

(13) Miyazaki, M.; Nakamura, H.; Maeda, H. *Chem. Lett.* **2001**, *30*, 442–443.

(14) (a) Tanaka, Y.; Slyadnev, M. N.; Sato, K.; Tokeshi, M.; Kim, H.; Kitamori, T. *Anal. Sci.* **2001**, *17*, 809–810. (b) Kanno, K.; Maeda, H.; Izumo, S.; Ikuno, M.; Takeshita, K.; Tashiro, A.; Fujii, M. *Lab Chip* **2002**, *2*, 15–18.

(15) Lottenberg, R.; Christensen, U.; Jackson, C. M.; Coleman, P. L. *Methods Enzymol.* **1981**, *80*, 341–361.

(16) Voet, D.; Voet, J. G., Biochemistry; John Wiley and Sons: New York, 2nd edn, 1995.

(17) (a) Craig, D. B.; Arriaga, E. A.; Wong, J. C. Y.; Lu, H.; Dovichi, N. J. *J. Am. Chem. Soc.* **1996**, *118*, 5245–5253. (b) Goodwin, M. G.; Avezoux, A.; Dales, S. L.; Anthony, C. *Biochem. J.* **1996**, *319*, 839–842.

(18) (a) Manz, A.; Becker, H. *Microsystem Technology in Chemistry and Life Sciences*; Springer: Berlin, 1998. (b) Yamaguchi, Y.; Takagi, F.; Yamashita, K.; Maeda, H. *AIChE J.* **2004**, *50*, 1530–1535.

(19) Urban, P. L.; Goodall, D. M.; Bruce, N. C. *Biotechnol. Adv.* **2006**, *24*, 42–57.

(20) Olsen, K.; Otte, J.; Skibsted, L. H. *J. Agric. Food Chem.* **2000**, *48*, 3086–3089.

JP808572A